Supplementary Information (SI)

Bridging-Arylene Effects on Spectroscopic and Photophysical Properties of Arylborane–Dipyrrinato Zinc(II) Complexes

Koyo Takaki,[a] Eri Sakuda,[a]* Akitaka Ito,[b] Shinnosuke Horiuchi,[a] Yasuhiro Arikawa[a] and Keisuke Umakoshi[a]*

[a]*Division of Chemistry and Materials Science, Graduate School of Engineering, Nagasaki University, Bunkyo-machi 1-14, Nagasaki 852-8521, Japan*

[b]*Graduate School of Engineering, Kochi University of Technology, Miyanokuchi 185, Tosayamada, Kami, Kochi 782-8502, Japan*

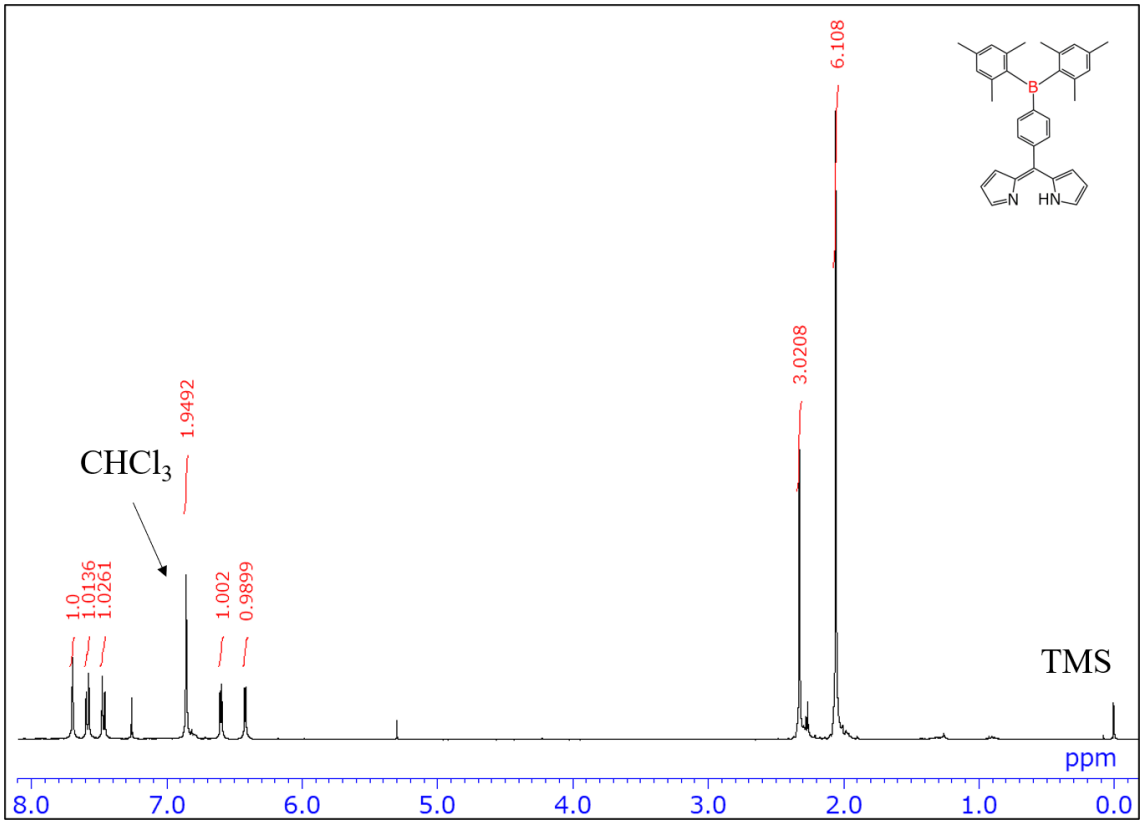

Figure S1. ^{1}H NMR spectra of 5-{4-(dimesitylboryl)phenyl}dipyrrin in $CDCl_3$ at 298 K.

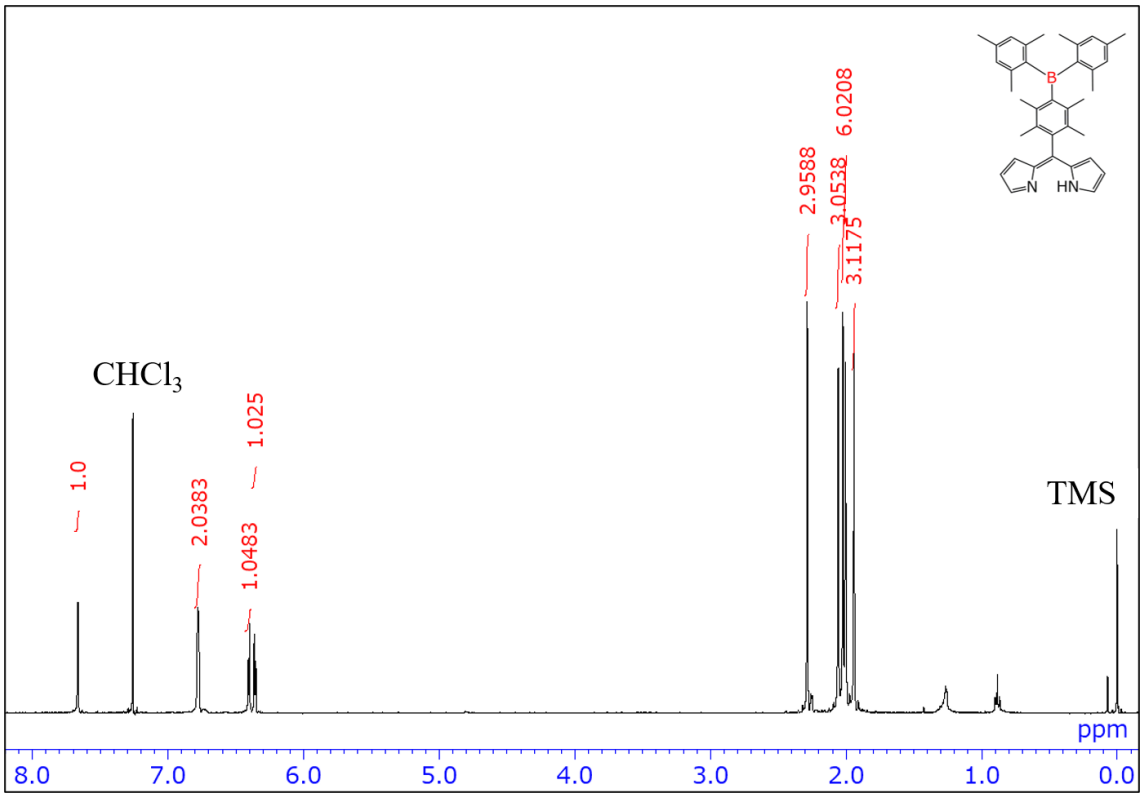

Figure S2. ^{1}H NMR spectra of **3** in $CDCl_3$ at 298 K.

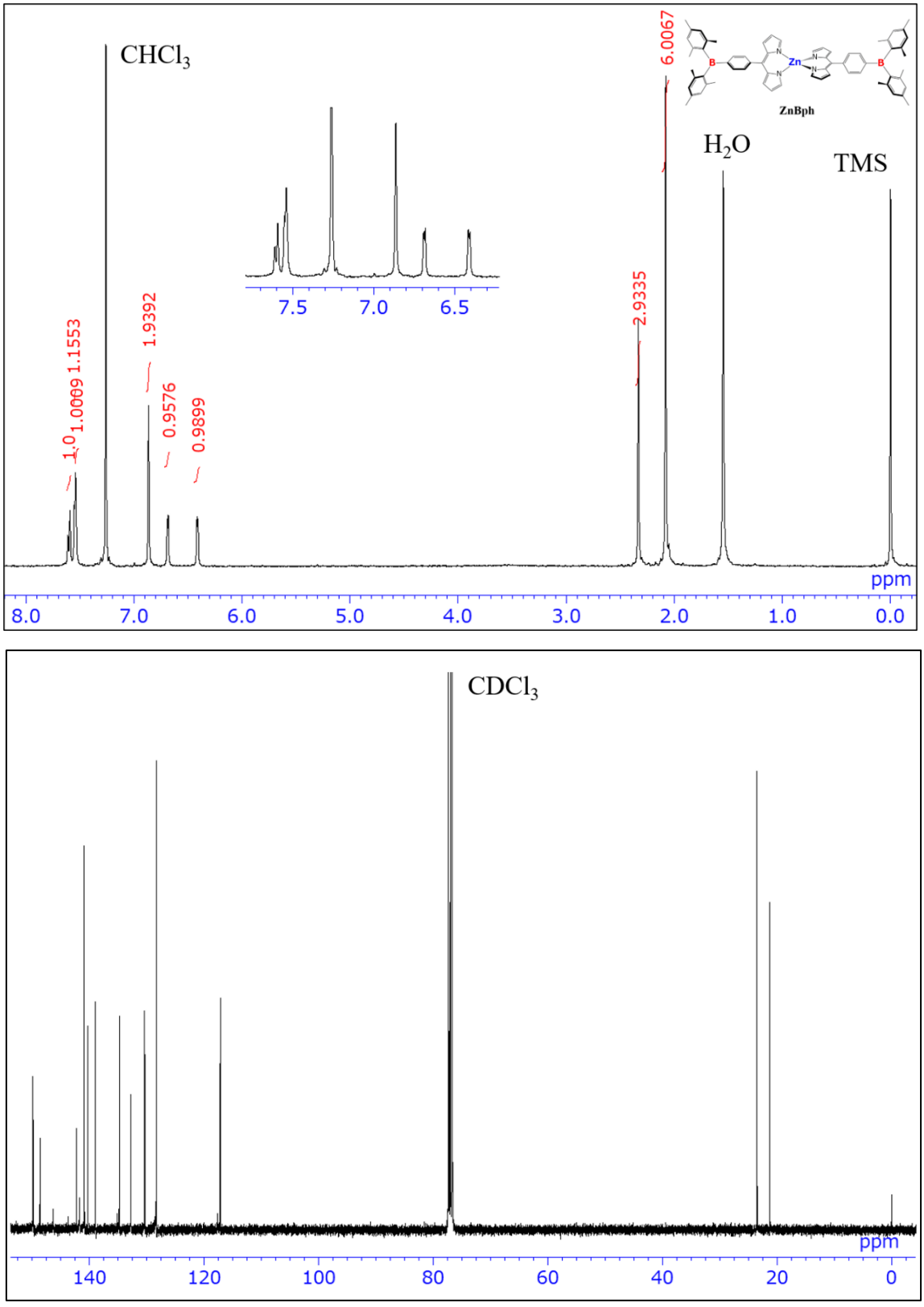

Figure S3. ^{1}H (top) and ^{13}C{^{1}H} NMR spectra (bottom) of **ZnBph** in $CDCl_3$ at 298 K.

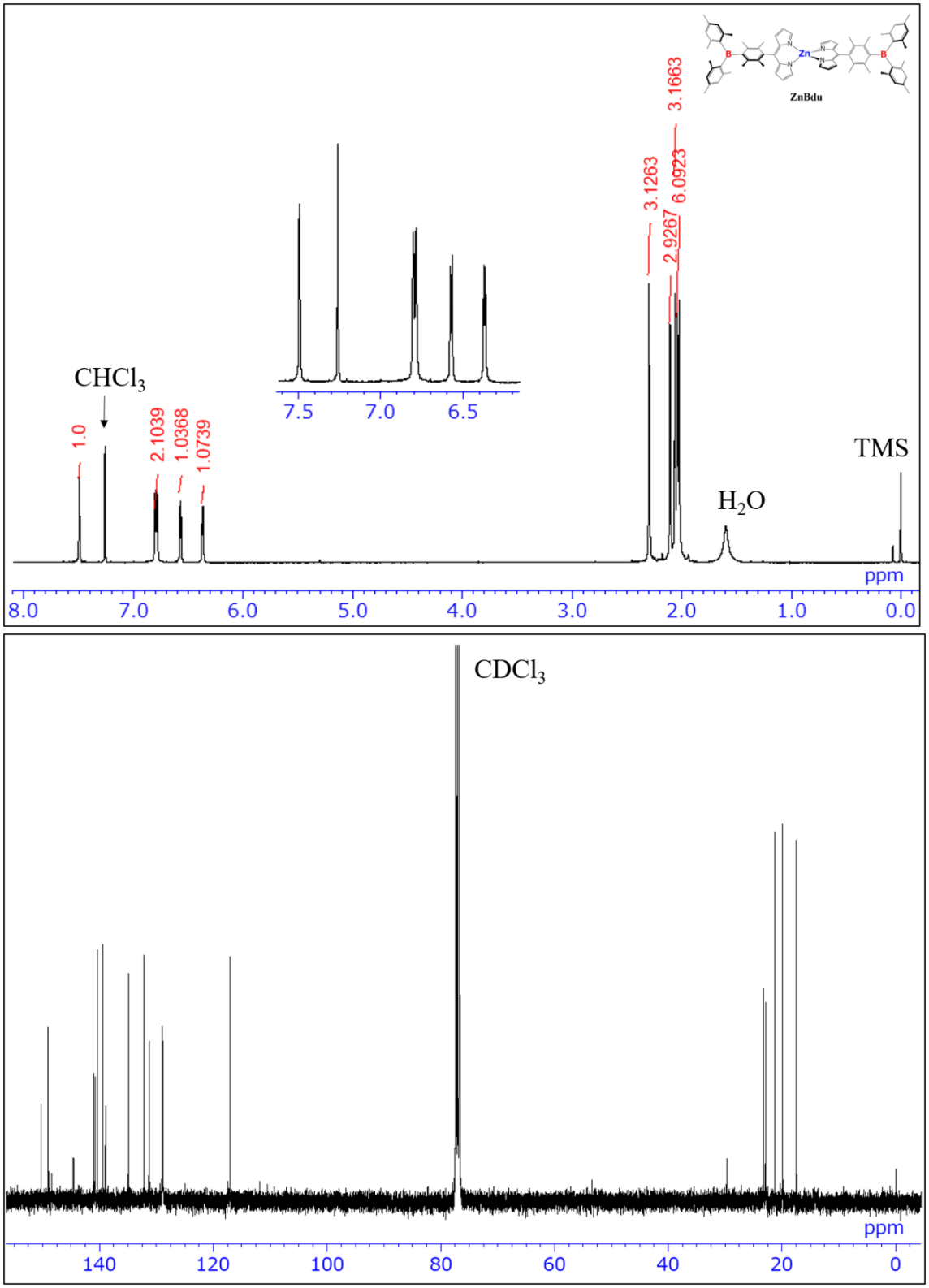

Figure S4. ^{1}H (top) and ^{13}C{^{1}H} NMR spectra (bottom) of **ZnBdu** in $CDCl_3$ at 298 K.

Table S1. Crystallographic Data for **ZnBdu**.

formula	$C_{74}H_{80}B_2N_4Zn$
fw	1112.47
crystal system	cubic
space group	$I\bar{4}3d$ (#220)
color of crystal	orange
crystal size (mm)	0.13 × 0.11 × 0.11
a (Å)	26.536(4)
b (Å)	26.536(4)
c (Å)	26.536(4)
α (deg)	90
β (deg)	90
γ (deg)	90
V (Å^3)	18686(4)
Z	12
ρ_{calc} (g cm^{-3})	1.186
μ(Mo Kα) (cm^{-1})	4.402
F(000)	7104.00
$2\theta_{max}$ (deg)	52.0
no. of all reflns collected	66863
no. of all unique reflns	3075
R_{int}	0.1121
no. of obsd reflns [a]	3072
no. of parameters	190
R_1 [a,b]	0.0587
wR_2 (all data)[c]	0.1209
GOF (all data)[d]	1.280
CCDC number	2035525

[a] $I > 2\sigma(I)$. [b] $R_1 = \Sigma\, ||F_o| - |F_c||/\Sigma\, |F_o|$.

[c] $wR_2 = \{\Sigma w(F_o^2 - F_c^2)^2/\Sigma w(F_o^2)^2\}^{1/2}$.

[d] GOF = $[\{\Sigma w(F_o^2 - F_c^2)^2/(N_o - N_v)]^{1/2}$, where N_o and N_v denote the number of observations and variables, respectively.

Table S2. Calculated Excited States of **ZnBph**.

Excited State	Transition	Energy (Wavelength)	Oscillator Strength
S_1	MO255 → MO256 (66%) MO255 → MO257 (34%)	2.6473 eV (468.35 nm)	0.0005
S_2	MO254 → MO257 (47%) MO255 → MO257 (53%)	2.6516 eV (467.59 nm)	0.0004
S_3	MO254 → MO256 (22%) MO254 → MO257 (38%) MO255 → MO256 (40%)	2.9424 eV (421.37 nm)	0.3013
S_4	MO254 → MO256 (40%) MO254 → MO259 (12%) MO255 → MO257 (48%)	2.9729 eV (417.04 nm)	0.3694
S_5	MO253 → MO256 (62%) MO253 → MO257 (38%)	3.2874 eV (377.15 nm)	0.0641
S_6	MO253 → MO256 (13%) MO254 → MO258 (37%) MO255 → MO256 (9%) MO255 → MO258 (41%)	3.3077 eV (374.84 nm)	0.1594
S_7	MO252 → MO256 (26%) MO252 → MO259 (18%) MO255 → MO259 (56%)	3.3382 eV (371.42 nm)	0.1662
S_8	MO252 → MO257 (65%) MO255 → MO259 (35%)	3.3528 eV (369.80 nm)	0.0726
S_9	MO250 → MO256 (53%) MO250 → MO257 (33%) MO251 → MO256 (14%)	3.3887 eV (365.88 nm)	0.2798
S_{10}	MO249 → MO257 (12%) MO250 → MO256 (22%) MO250 → MO257 (13%) MO251 → MO257 (53%)	3.3983 eV (364.84 nm)	0.0708
S_{11}	MO254 → MO258	3.4410 eV (360.31 nm)	0.0003
S_{12}	MO249 → MO257	3.4899 eV (355.27 nm)	0.0322
S_{13}	MO248 → MO256 (62%) MO248 → MO257 (38%)	3.4931 eV (354.94 nm)	0.0422
S_{14}	MO254 → MO259 (52%) MO255 → MO259 (48%)	3.4988 eV (354.36 nm)	0.0001
S_{15}	MO245 → MO256 (32%) MO246 → MO256 (30%) MO246 → MO257 (18%) MO247 → MO257 (20%)	3.5618 eV (348.10 nm)	0.0387
S_{16}	MO244 → MO257 (9%) MO245 → MO257 (15%)	3.5646 eV (347.82 nm)	0.0164

	MO246 → MO256 (30%) MO246 → MO257 (19%) MO247 → MO256 (18%) MO247 → MO259 (9%)		
S_{17}	MO245 → MO256 (52%) MO245 → MO257 (27%) MO247 → MO256 (21%)	3.5712 eV (347.18 nm)	0.0337
S_{18}	MO245 → MO257 (22%) MO247 → MO257 (15%) MO253 → MO257 (63%)	3.5814 eV (346.19 nm)	0.0158
S_{19}	MO244 → MO257 (18%) MO245 → MO257 (42%) MO247 → MO257 (25%) MO253 → MO256 (15%)	3.5858 eV (345.76 nm)	0.0998
S_{20}	MO252 → MO256 (60%) MO252 → MO257 (40%)	3.6085 eV (343.59 nm)	0.0015
S_{21}	MO251 → MO256 (60%) MO251 → MO257 (40%)	3.6465 eV (340.01 nm)	0.0012
S_{22}	MO243 → MO256 (76%) MO250 → MO257 (24%)	3.6664 eV (338.17 nm)	0.0886
S_{23}	MO242 → MO257 (17%) MO250 → MO257 (83%)	3.6708 eV (337.76 nm)	0.0059
S_{24}	MO242 → MO257 (20%) MO243 → MO257 (80%)	3.6946 eV (335.58 nm)	0.0006
S_{25}	MO249 → MO256 (59%) MO249 → MO257 (41%)	3.7063 eV (334.53 nm)	0.0000
S_{26}	MO248 → MO257	3.7391 eV (331.59 nm)	0.0001
S_{27}	MO253 → MO256 (21%) MO253 → MO257 (16%) MO253 → MO258 (63%)	3.7417 eV (331.36 nm)	0.0635
S_{28}	MO244 → MO256 (52%) MO245 → MO256 (16%) MO245 → MO257 (32%)	3.7573 eV (329.98 nm)	0.0039
S_{29}	MO244 → MO257 (66%) MO245 → MO256 (34%)	3.7645 eV (329.35 nm)	0.0045
S_{30}	MO244 → MO256 (10%) MO247 → MO256 (53%) MO247 → MO257 (37%)	3.7855 eV (327.53 nm)	0.0001
S_{31}	MO246 → MO257	3.8097 eV (325.45 nm)	0.0007
S_{32}	MO252 → MO257 (25%) MO252 → MO259 (75%)	3.8118 eV (325.27 nm)	0.0723
S_{33}	MO242 → MO256 (31%) MO242 → MO257 (24%)	3.8383 eV (323.02 nm)	0.0060

	MO243 → MO256 (27%) MO243 → MO257 (18%)		
S_{34}	MO242 → MO257 (69%) MO243 → MO256 (31%)	3.8428 eV (322.64 nm)	0.0039
S_{35}	MO250 → MO256 (16%) MO250 → MO257 (12%) MO250 → MO258 (72%)	3.8666 eV (320.65 nm)	0.0007
S_{36}	MO240 → MO256 (20%) MO241 → MO256 (12%) MO249 → MO259 (11%) MO251 → MO259 (57%)	3.8900 eV (318.73 nm)	0.0128
S_{37}	MO241 → MO256 (46%) MO241 → MO257 (27%) MO250 → MO256 (11%) MO250 → MO258 (16%)	3.8957 eV (318.26 nm)	0.2376
S_{38}	MO240 → MO257 (42%) MO241 → MO257 (12%) MO251 → MO257 (14%) MO251 → MO259 (32%)	3.9211 eV (316.20 nm)	0.1703
S_{39}	MO241 → MO256 (12%) MO248 → MO256 (16%) MO248 → MO257 (12%) MO248 → MO258 (60%)	3.9606 eV (313.05 nm)	0.0808
S_{40}	MO249 → MO257 (21%) MO249 → MO259 (79%)	3.9719 eV (312.15 nm)	0.0391
S_{41}	MO238 → MO256 (12%) MO238 → MO257 (12%) MO239 → MO256 (48%) MO239 → MO257 (28%)	4.0049 eV (309.58 nm)	0.0306
S_{42}	MO238 → MO257	4.0198 eV (308.44 nm)	0.0146
S_{43}	MO238 → MO256 (7%) MO239 → MO256 (17%) MO239 → MO257 (12%) MO246 → MO256 (12%) MO246 → MO257 (9%) MO246 → MO258 (43%)	4.0239 eV (308.12 nm)	0.0013
S_{44}	MO238 → MO257 (16%) MO247 → MO257 (17%) MO247 → MO259 (67%)	4.0507 eV (306.08 nm)	0.0195
S_{45}	MO241 → MO257	4.2024 eV (295.04 nm)	0.0001
S_{46}	MO240 → MO256 (59%) MO240 → MO257 (41%)	4.2077 eV (294.66 nm)	0.0001
S_{47}	MO252 → MO258	4.2791 eV (289.75 nm)	0.0000

S_{48}	MO253 → MO259	4.3045 eV (288.03 nm)	0.0000
S_{49}	MO251 → MO258	4.3204 eV (286.97 nm)	0.0000
S_{50}	MO245 → MO258	4.3250 eV (286.67 nm)	0.0014

HOMO: MO255, LUMO: MO256

Table S3. Molecular-Orbital Contributions of **ZnBph**.

Molecular Orbital	Eigenvalue / Hartrees	MO Contribution / %				
		zinc	Bph-dipy			
			dipyrrinate	phenylene	boron	mesityl
259 (LUMO+3)	−0.05902	0.14	17.44	27.27	25.60	29.55
258 (LUMO+2)	−0.06117	0.15	18.32	23.16	24.29	34.08
257 (LUMO+1)	−0.08369	0.49	76.99	14.58	3.83	4.11
256 (LUMO)	−0.08438	0.55	76.78	14.41	3.85	4.41
255 (HOMO)	−0.19805	0.02	96.35	3.54	0.01	0.08
254 (HOMO–1)	−0.19870	0.01	96.68	3.22	0.01	0.08
253 (HOMO–2)	−0.22306	0.00	0.13	11.07	1.36	87.44
252 (HOMO–3)	−0.22428	0.00	0.21	11.02	1.28	87.49

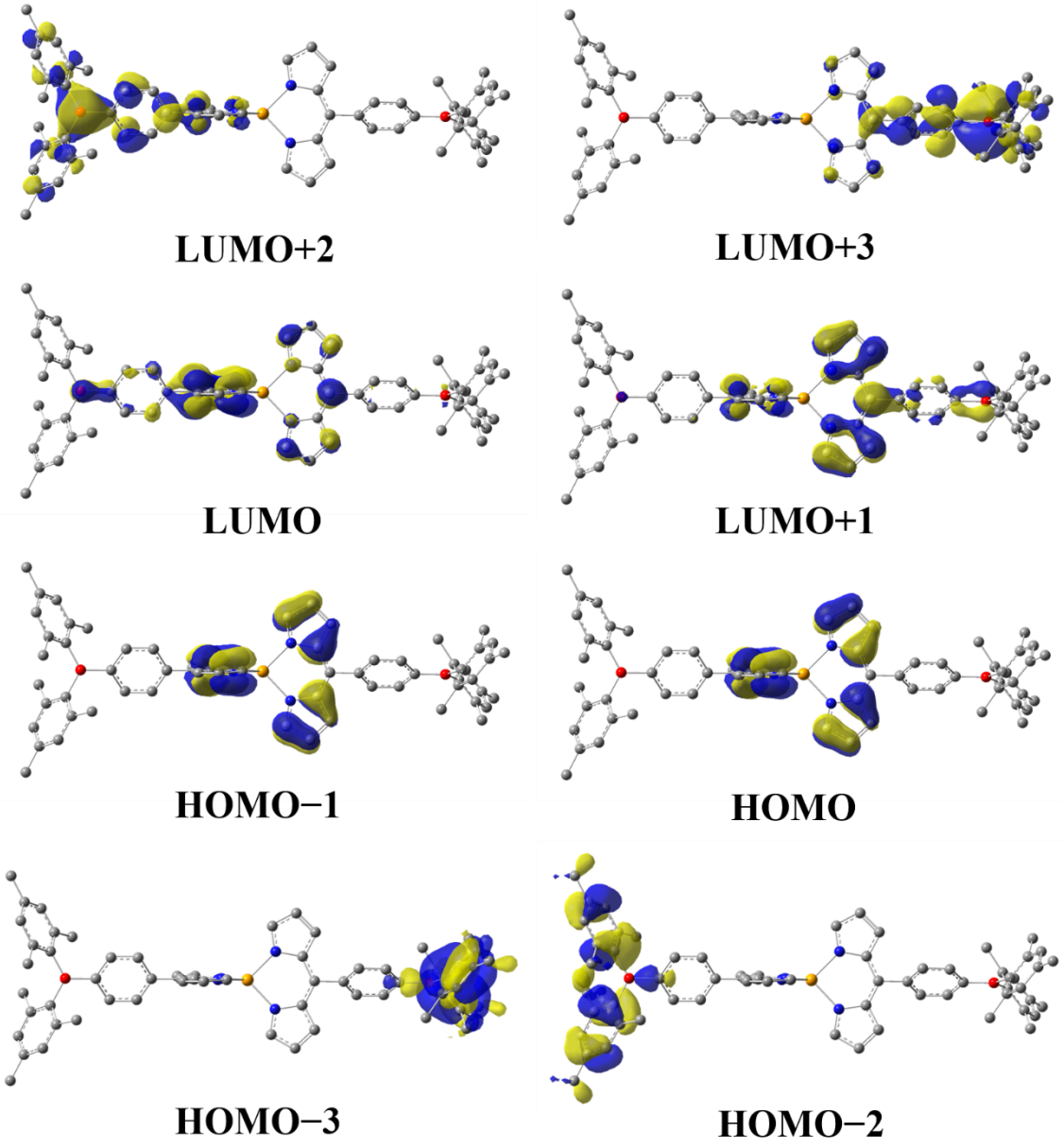

Figure S5. Kohn–Sham molecular orbitals of **ZnBph**.

Table S4. Calculated Excited States of **ZnBdu**.

Excited State	Transition	Energy (Wavelength)	Oscillator Strength
S_1	MO287 → MO288	2.7222 eV (455.45 nm)	0.0000
S_2	MO286 → MO288 (10%) MO286 → MO289 (48%) MO287 → MO289 (42%)	2.7258 eV (454.86 nm)	0.0000
S_3	MO284 → MO288 (20%) MO286 → MO288 (38%) MO286 → MO289 (21%) MO287 → MO288 (21%)	3.0648 eV (404.54 nm)	0.3419
S_4	MO286 → MO289	3.0747 eV (403.24 nm)	0.3580
S_5	MO282 → MO289 (18%) MO284 → MO288 (58%) MO287 → MO289 (24%)	3.2098 eV (386.26 nm)	0.1475
S_6	MO284 → MO288 (32%) MO285 → MO288 (16%) MO285 → MO289 (35%) MO286 → MO289 (17%)	3.2147 eV (385.68 nm)	0.1858
S_7	MO280 → MO288 (22%) MO281 → MO288 (13%) MO281 → MO289 (65%)	3.2883 eV (377.05 nm)	0.0007
S_8	MO280 → MO288	3.2883 eV (377.05 nm)	0.0000
S_9	MO286 → MO290 (52%) MO287 → MO290 (48%)	3.3230 eV (373.11 nm)	0.0009
S_{10}	MO287 → MO291	3.3279 eV (372.56 nm)	0.0008
S_{11}	MO287 → MO290	3.4882 eV (355.44 nm)	0.0000
S_{12}	MO286 → MO291 (56%) MO287 → MO291 (44%)	3.4963 eV (354.62 nm)	0.0000
S_{13}	MO285 → MO288	3.5395 eV (350.29 nm)	0.0002
S_{14}	MO284 → MO288 (15%) MO284 → MO289 (70%) MO285 → MO289 (15%)	3.5421 eV (350.03 nm)	0.0001
S_{15}	MO283 → MO288 (74%) MO284 → MO288 (26%)	3.5500 eV (349.25 nm)	0.0004
S_{16}	MO282 → MO288 (14%) MO282 → MO289 (64%) MO285 → MO289 (22%)	3.5512 eV (349.14 nm)	0.0041
S_{17}	MO283 → MO290 (64%) MO284 → MO290 (36%)	3.6154 eV (342.93 nm)	0.1603
S_{18}	MO282 → MO291 (63%) MO285 → MO291 (37%)	3.6230 eV (342.21 nm)	0.1828

S_{19}	MO280 → MO290	3.6645 eV (338.34 nm)	0.3213
S_{20}	MO280 → MO290 (37%) MO281 → MO291 (63%)	3.6703 eV (337.80 nm)	0.0200
S_{21}	MO284 → MO290 (82%) MO285 → MO290 (18%)	3.6871 eV (336.26 nm)	0.0020
S_{22}	MO272 → MO288 (12%) MO273 → MO289 (11%) MO282 → MO288 (60%) MO285 → MO288 (17%)	3.6906 eV (335.95 nm)	0.0128
S_{23}	MO282 → MO288 (9%) MO283 → MO288 (10%) MO283 → MO289 (43%) MO284 → MO289 (13%) MO285 → MO291 (25%)	3.6912 eV (335.89 nm)	0.0205
S_{24}	MO285 → MO291	3.6921 eV (335.81 nm)	0.0004
S_{25}	MO281 → MO288	3.6938 eV (335.66 nm)	0.0002
S_{26}	MO273 → MO288 (62%) MO282 → MO288 (38%)	3.6958 eV (335.48 nm)	0.0613
S_{27}	MO272 → MO288 (23%) MO280 → MO289 (77%)	3.6972 eV (335.35 nm)	0.0658
S_{28}	MO272 → MO289 (11%) MO273 → MO288 (13%) MO273 → MO289 (15%) MO280 → MO288 (9%) MO280 → MO289 (43%) MO283 → MO289 (9%)	3.6973 eV (335.34 nm)	0.0227
S_{29}	MO270 → MO288	3.7692 eV (328.94 nm)	0.0870
S_{30}	MO279 → MO288 (18%) MO279 → MO289 (82%)	3.7856 eV (327.51 nm)	0.0005
S_{31}	MO278 → MO288	3.7864 eV (327.44 nm)	0.0000
S_{32}	MO270 → MO289 (10%) MO274 → MO288 (14%) MO275 → MO289 (18%) MO276 → MO288 (17%) MO277 → MO289 (19%) MO280 → MO288 (10%) MO281 → MO289 (12%)	3.7973 eV (326.51 nm)	0.0000
S_{33}	MO274 → MO288 (33%) MO276 → MO288 (42%) MO280 → MO288 (25%)	3.7986 eV (326.40 nm)	0.0012
S_{34}	MO270 → MO288 (18%) MO271 → MO288 (12%) MO271 → MO289 (18%)	3.8008 eV (326.21 nm)	0.0000

	MO274 → MO288 (9%) MO275 → MO289 (8%) MO276 → MO288 (12%) MO277 → MO289 (10%) MO280 → MO288 (7%) MO281 → MO289 (6%)		
S_{35}	MO275 → MO288 (18%) MO275 → MO289 (82%)	3.8664 eV (320.67 nm)	0.0020
S_{36}	MO274 → MO288	3.8671 eV (320.61 nm)	0.0009
S_{37}	MO272 → MO288 (62%) MO273 → MO288 (38%)	3.8690 eV (320.45 nm)	0.0045
S_{38}	MO272 → MO288 (18%) MO272 → MO289 (82%)	3.8723 eV (320.18 nm)	0.0044
S_{39}	MO278 → MO289 (14%) MO278 → MO290 (86%)	3.9054 eV (317.47 nm)	0.0449
S_{40}	MO279 → MO288 (59%) MO279 → MO291 (41%)	3.9086 eV (317.21 nm)	0.0148
S_{41}	MO279 → MO291	3.9109 eV (317.02 nm)	0.0314
S_{42}	MO278 → MO288 (17%) MO278 → MO289 (83%)	3.9128 eV (316.87 nm)	0.0012
S_{43}	MO271 → MO288	3.9179 eV (316.45 nm)	0.0001
S_{44}	MO270 → MO289 (54%) MO271 → MO288 (32%) MO271 → MO289 (14%)	3.9230 eV (316.04 nm)	0.0000
S_{45}	MO275 → MO288 (42%) MO277 → MO288 (47%) MO281 → MO288 (11%)	3.9584 eV (313.22 nm)	0.0000
S_{46}	MO274 → MO289 (35%) MO276 → MO288 (9%) MO276 → MO289 (45%) MO280 → MO289 (11%)	3.9615 eV (312.97 nm)	0.0000
S_{47}	MO276 → MO290	3.9805 eV (311.48 nm)	0.0419
S_{48}	MO277 → MO288 (18%) MO277 → MO291 (82%)	3.9852 eV (311.11 nm)	0.0303
S_{49}	MO275 → MO288 (72%) MO277 → MO291 (28%)	3.9887 eV (310.84 nm)	0.0031
S_{50}	MO274 → MO288 (17%)	3.9918 eV (310.59 nm)	0.0003

HOMO: MO287, LUMO: MO288

Table S5. Molecular-Orbital Contributions of **ZnBdu**.

Molecular Orbital	Eigenvalue / Hartrees	MO Contribution / %				
		zinc	Bdu-dipy			
			dipyrrinate	durylene	boron	mesityl
291 (LUMO+3)	−0.05883	0.01	2.00	16.16	30.35	51.48
290 (LUMO+2)	−0.05905	0.01	2.00	16.54	30.27	51.18
289 (LUMO+1)	−0.07798	0.58	90.58	8.79	0.01	0.04
288 (LUMO)	−0.07804	0.59	90.54	8.85	0.00	0.02
287 (HOMO)	−0.19579	0.00	97.29	2.67	0.01	0.03
286 (HOMO–1)	−0.19621	0.00	97.33	2.63	0.01	0.03
285 (HOMO–2)	−0.21959	0.00	3.08	81.43	0.32	15.17
284 (HOMO–3)	−0.21963	0.01	2.88	81.04	0.34	15.73

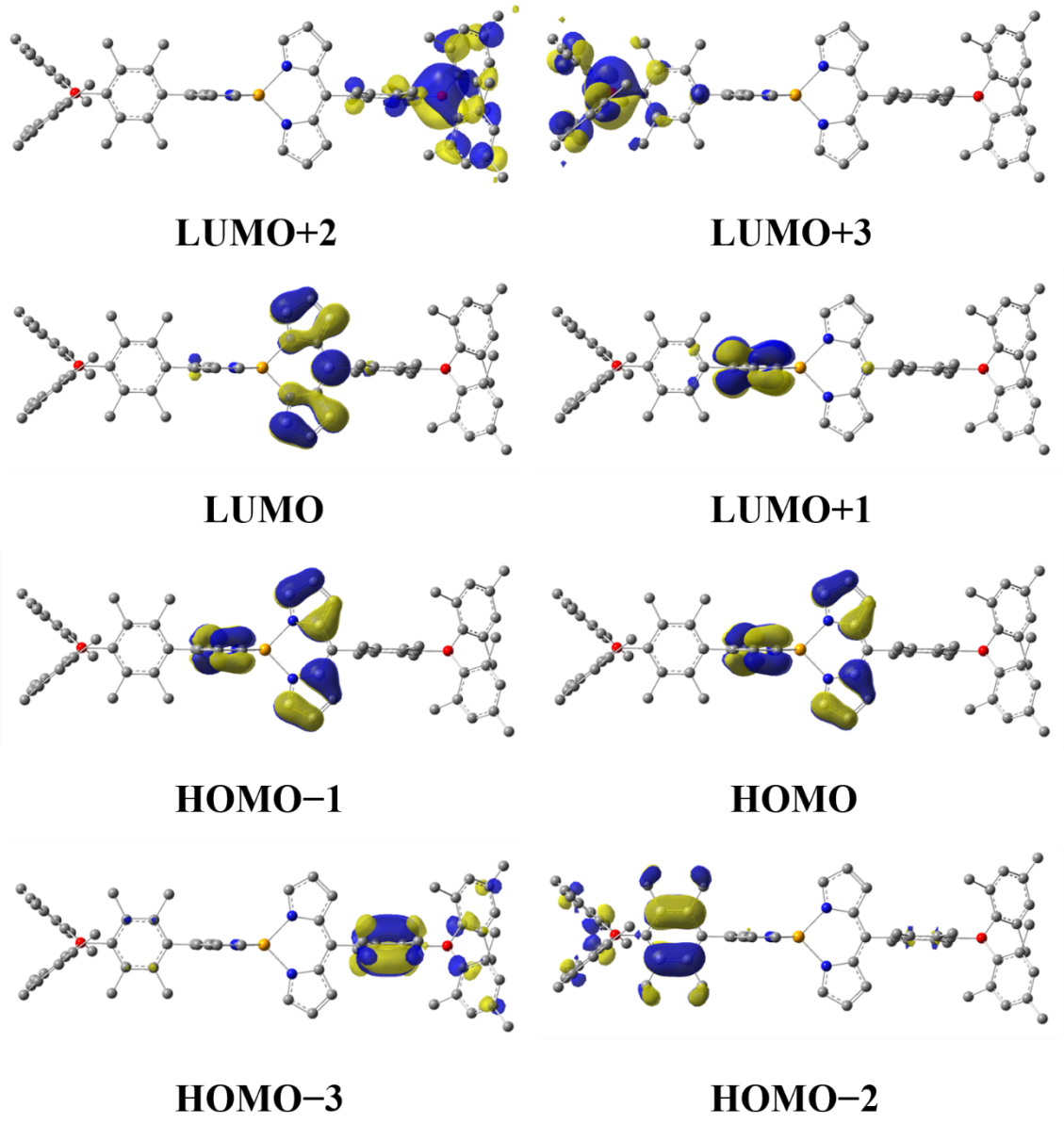

Figure S6. Kohn–Sham molecular orbitals of **ZnBdu**.

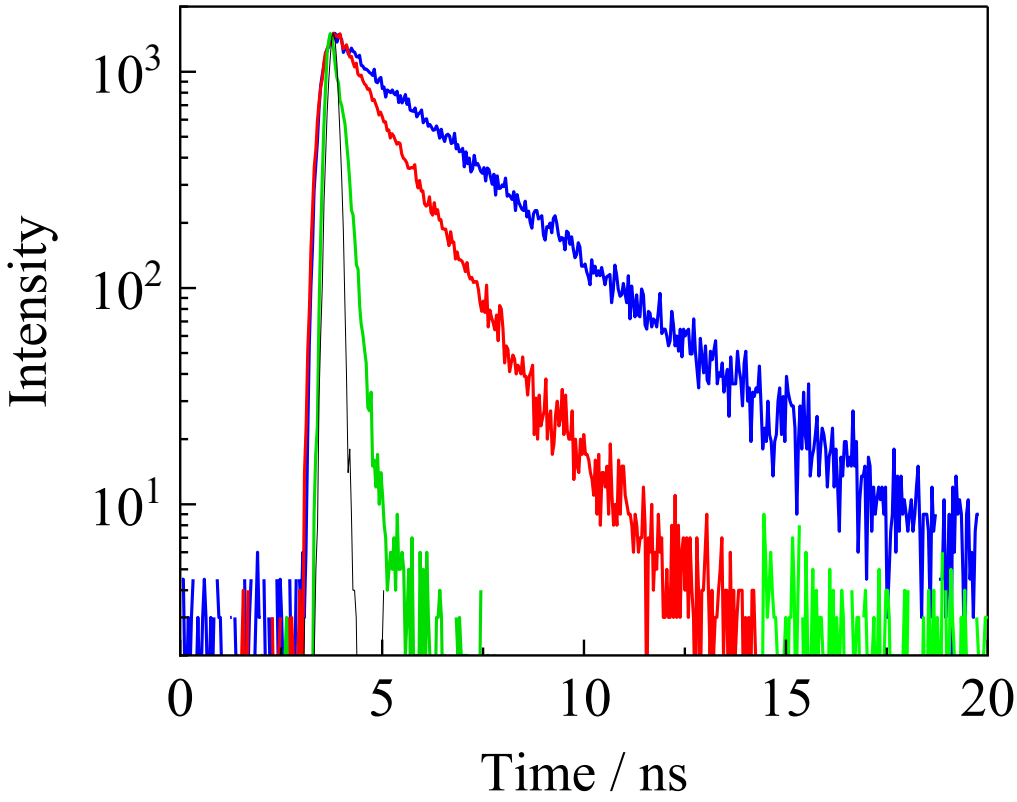

Figure S7. Fluorescence decay profiles of **ZnBph** (red), **ZnBdu** (blue) and **ZnBph·2F**$^-$ (green) in toluene at 298 K. Black curve represents instrumental response function.

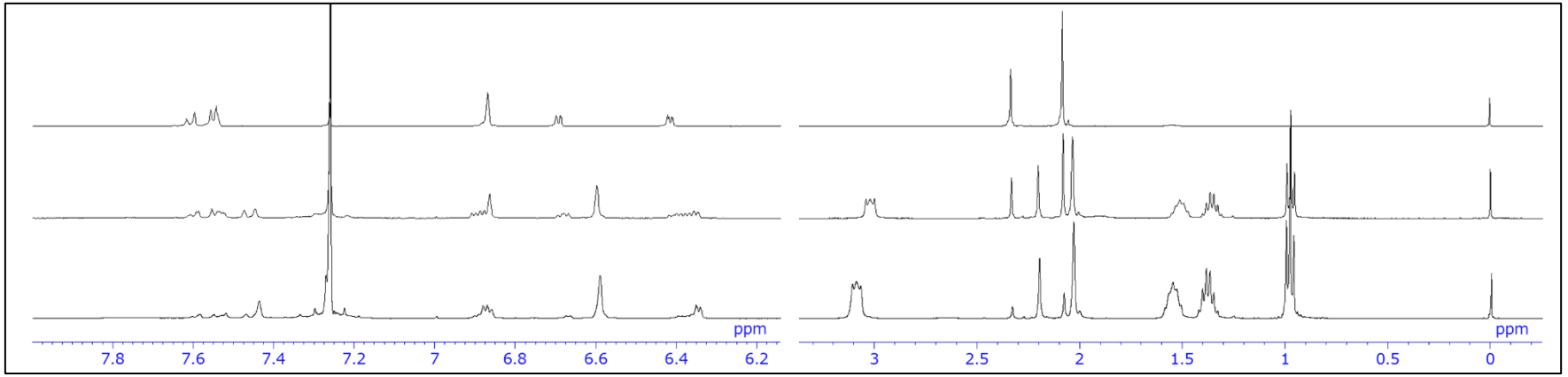

Figure S8. ^{1}H NMR spectra (400 MHz, $CDCl_3$) of **ZnBph** in the absence (top) and presence (2 equiv. and 4 equiv.) of TBAF (middle and bottom, respectively).

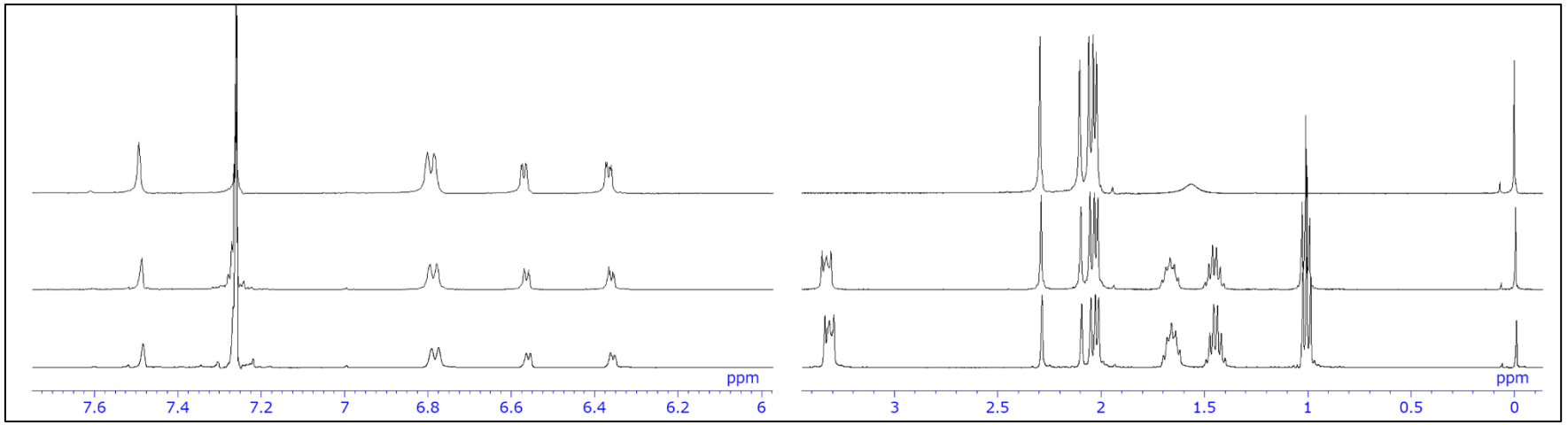

Figure S9. ^{1}H NMR spectra (400 MHz, $CDCl_3$) of **ZnBdu** in the absence (top) and presence (2 equiv. and 4 equiv.) of TBAF (middle and bottom, respectively).

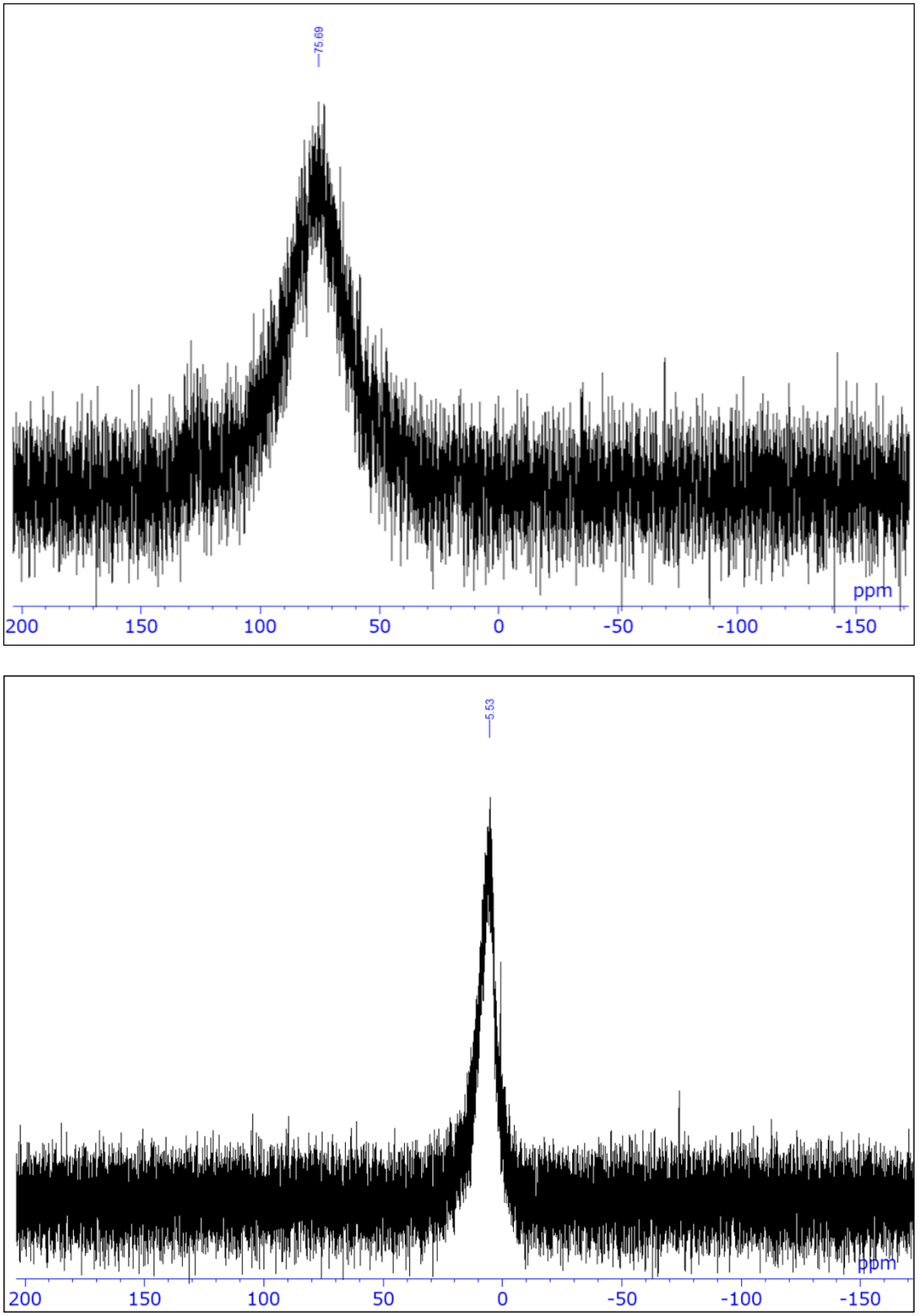

Figure S10. $^{11}B\{^{1}H\}$ NMR spectra (400 MHz, $CDCl_3$) of **ZnBph** in the absence (top) and presence (4.0 equiv.) of TBAF (bottom).

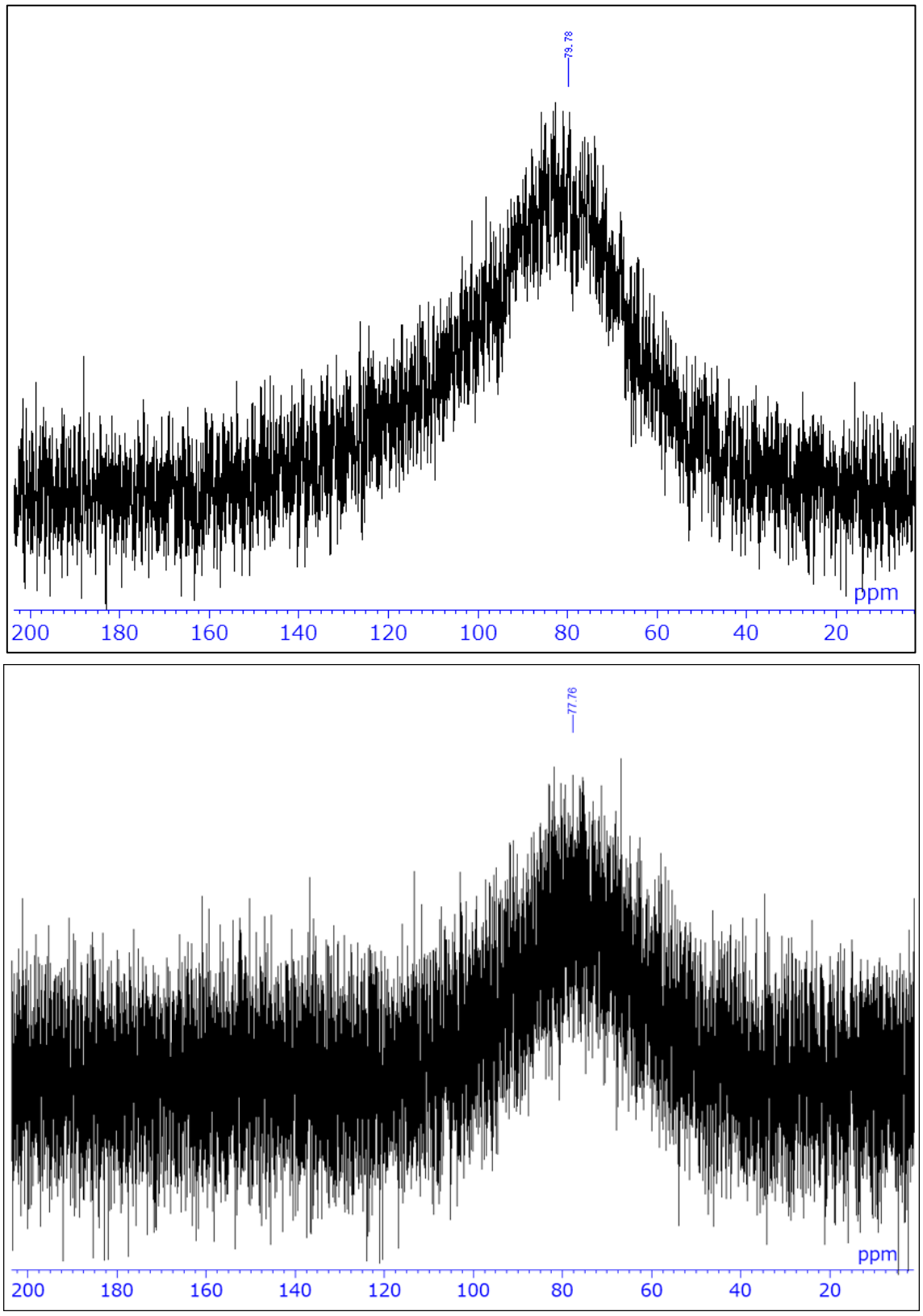

Figure S11. $^{11}B\{^{1}H\}$ NMR spectra (400 MHz, $CDCl_3$) of **ZnBdu** in the absence (top) and presence (4.0 equiv.) of TBAF (bottom).

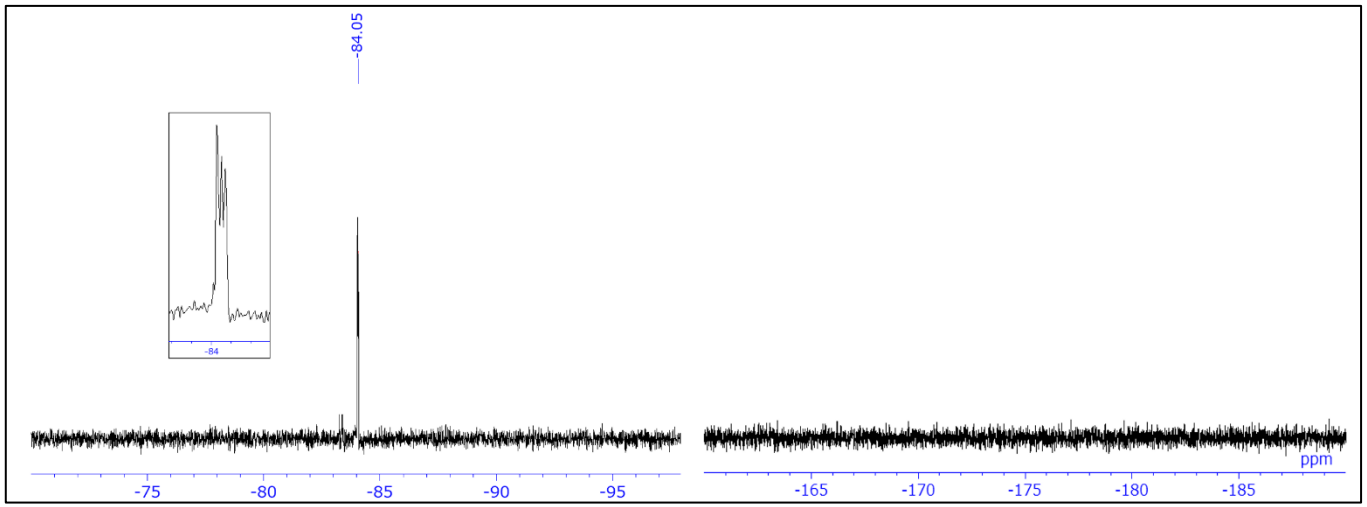

Figure S12. $^{19}F\{^{1}H\}$ NMR spectrum (400 MHz, $CDCl_3$) of TBAF (existing as $CDClF_2$).

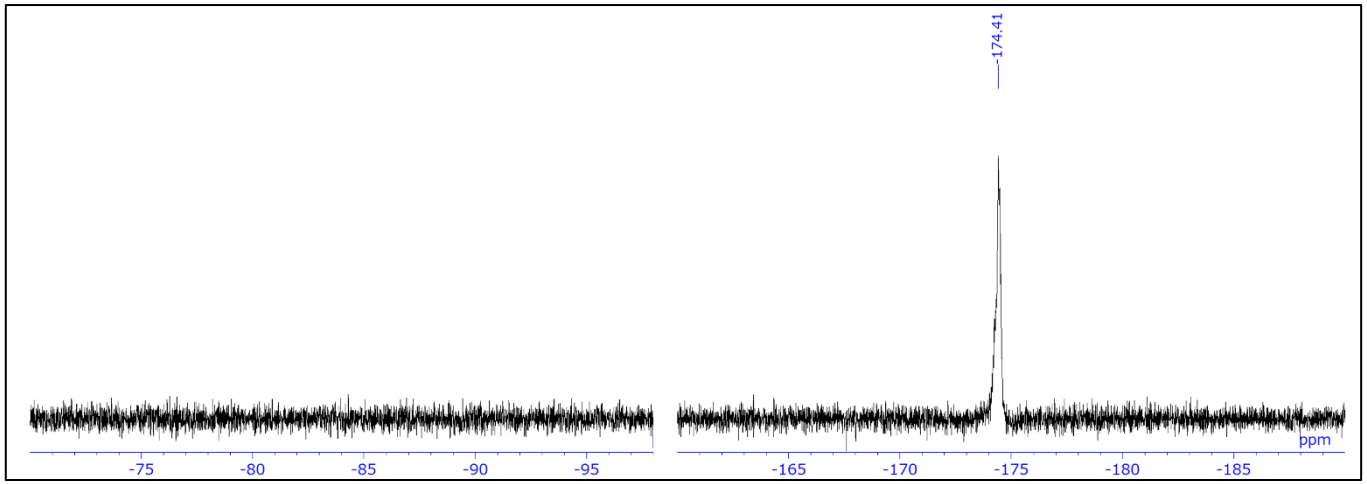

Figure S13. $^{19}F\{^{1}H\}$ NMR spectrum (400 MHz, $CDCl_3$) of **ZnBph** in the presence of TBAF (4.0 equiv.).

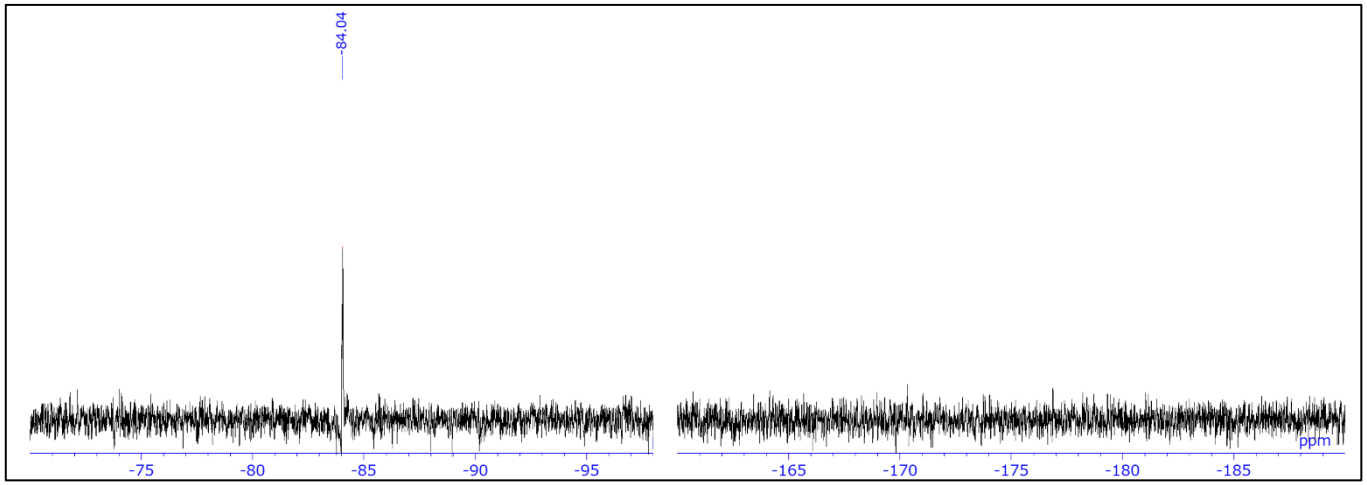

Figure S14. $^{19}F\{^{1}H\}$ NMR spectrum (400 MHz, $CDCl_3$) of **ZnBdu** in the presence of TBAF (4.0 equiv.).

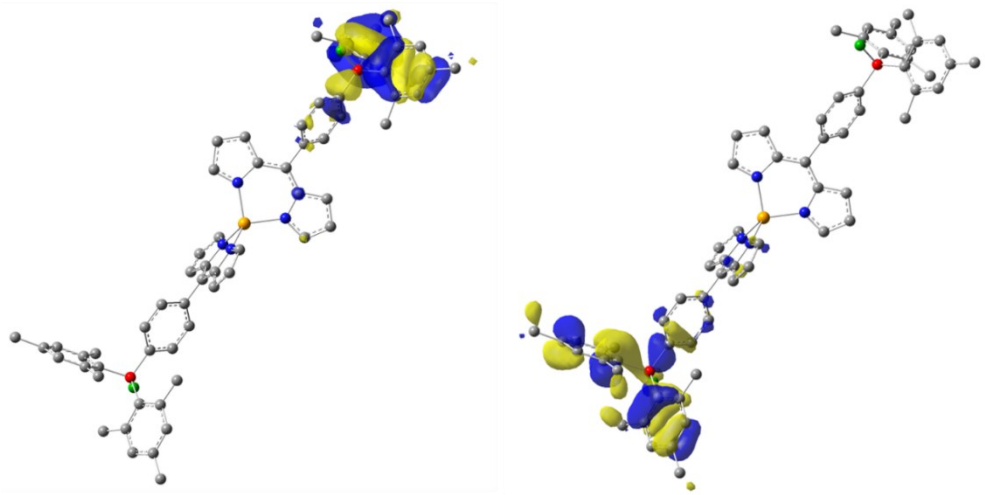

Figure S15. Kohn–Sham molecular orbitals of **ZnBph·2F**$^{-}$.